Environment-Assisted Quantum Transport in Ordered Systems

Environment-assisted quantum transport in ordered systems

2012 New J. Phys. 14 053041

(http://iopscience.iop.org/1367-2630/14/5/053041)

New Journal of Physics
The open-access journal for physics

Environment-assisted quantum transport in ordered systems

Ivan Kassal[1,2,3] **and Alán Aspuru-Guzik**[2]

[1] School of Mathematics and Physics and Centre for Engineered Quantum Systems, The University of Queensland, St Lucia, QLD 4072, Australia
[2] Department of Chemistry and Chemical Biology, Harvard University, Cambridge, MA 02138, USA
E-mail: i.kassal@uq.edu.au

New Journal of Physics **14** (2012) 053041 (12pp)
Received 20 March 2012
Published 29 May 2012
Online at http://www.njp.org/
doi:10.1088/1367-2630/14/5/053041

Abstract. Noise-assisted transport in quantum systems occurs when quantum time evolution and decoherence conspire to produce a transport efficiency that is higher than what would be seen in either the purely quantum or purely classical cases. In disordered systems, it has been understood as the suppression of coherent quantum localization through noise, which brings detuned quantum levels into resonance and thus facilitates transport. We report several new mechanisms of environment-assisted transport in ordered systems, in which there is no localization to overcome and where one would naively expect that coherent transport is the fastest possible. Although we are particularly motivated by the need to understand excitonic energy transfer in photosynthetic light-harvesting complexes, our model is general—transport in a tight-binding system with dephasing, a source and a trap—and can be expected to have wider application.

[3] Author to whom any correspondence should be addressed.

Contents

Recent experimental studies of photosynthetic light-harvesting complexes have confronted us with the fact that at least some of these systems exhibit excitonic coherence that is surprisingly long considering their noisy environment [1–3]. This makes it clear that if we are to understand their high light-harvesting efficiency, we must study the ways in which quantum transport is affected by the interplay of coherence and noise [4–21]. It has been found that noise can enhance quantum transport in model excitonic Hamiltonians [4–6], a phenomenon called environment-assisted quantum transport (ENAQT) or decoherence-assisted transport.

In the simplest approach, different environments around each chromophore lead to a tight-binding model with sites that have different energies (disorder). Because of disorder, the exciton becomes localized through coherent phenomena such as destructive interference or Anderson localization [4, 5, 8, 11]. ENAQT is then simple to understand: noise can destroy the coherent localization, helping the exciton reach the trap site and increasing the efficiency. Alternatively, decoherence has been described as fluctuations of site energies which can transiently bring levels into resonance, facilitating transport.

If these interpretations were the whole story, ENAQT would be impossible in ordered systems, those without energetic disorder. The absence of ENAQT in ordered linear chains was predicted at least twice: for example, Cao and Silbey predict 'the lack of environment-assistance in linear-chain systems' [12], while Plenio and Huelga note 'the expectation that noise does not enhance the transport of excitations' in uniform chains [5]. This expectation is strengthened by proofs of the impossibility of ENAQT in end-to-end transport in ordered chains [5, 12]. We revisit the ordered chain and show that the case of end-to-end transport is the *only* case where ENAQT is impossible: its absence in end-to-end transport is the rare exception that we are able to explain. We anticipate that these findings will shed light on the efficiency of transport in ordered excitonic systems, whether artificial, such as *J*-aggregates, or natural, such as the LHII complex in purple bacteria and the chlorosome in green sulfur bacteria.

Results related to ours were reported by Gaab and Bardeen [6]. They considered ordered systems and noted that the environment can sometimes enhance the 'effective trapping rate'. By contrast, we focus on the trapping efficiency, a measure of how often the exciton is productively

trapped as opposed to lost, regardless of how fast the transport is (loss is not modelled in [6], so the efficiency is always 1). We do not average over initial sites, which allows us to explain the absence of ENAQT in end-to-end transport.

1. The model and definition of environment-assisted quantum transport (ENAQT)

The ordered system we consider is a one-dimensional array of N identical sites, coupled to their nearest neighbours and described by the Hamiltonian

$$H_0 = V \sum_{m=1}^{N-1} \left(|m\rangle\langle m+1| + |m+1\rangle\langle m| \right), \tag{1}$$

where V is the coupling strength and $\hbar = 1$. This Hamiltonian is equivalent to a system of coupled two-level systems that is restricted to the single-excitation sector.

To study the efficiency of transport mediated by this Hamiltonian, we introduce two distinct attenuation mechanisms. Firstly, the particle is irreversibly *lost* from each site at an equal rate μ, modelling processes such as exciton recombination. Secondly, at a particular trap site $|\tau\rangle$, the particle can be *trapped* at a rate κ, modelling, for example, the transfer of an exciton to a photosynthetic reaction centre. These attenuation mechanisms are incorporated by adding a non-Hermitian part to the Hamiltonian,

$$H_{\text{atten}} = -\mathrm{i}\mu \sum_m |m\rangle\langle m| - \mathrm{i}\kappa\, |\tau\rangle\, \langle\tau|\,. \tag{2}$$

Loss and trapping both result in particle disappearance and have the same mathematical form; the distinction is that we consider the energy carried by lost particles to be unavailable and the trapped energy to be productively useable. The norm of the state at time t is the probability that the particle will survive that long.

The attenuation mechanisms continuously reduce the particle's survival probability, so that after a sufficiently long time, $t \gg \mu^{-1}$, the probability of finding the particle is negligible. If $\rho(t)$ is the system's density matrix at time t, the probability of trapping the particle in the interval $[t, t+\mathrm{d}t]$ is $2\kappa\, \langle\tau|\rho(t)|\tau\rangle\, \mathrm{d}t$. The efficiency of transport, for the initial state $\rho(0)$, is then the overall trapping probability,

$$\eta = 2\kappa \int_0^\infty \langle\tau|\rho(t)|\tau\rangle\, \mathrm{d}t. \tag{3}$$

Likewise, the probability of loss is $\eta' = 2\mu \sum_m \int_0^\infty \langle m|\rho(t)|m\rangle\, \mathrm{d}t = 2\mu \int_0^\infty \mathrm{tr}\,\rho(t)\, \mathrm{d}t$ and these branching ratios satisfy $\eta + \eta' = 1$.

Environmental effects are modelled as (Markovian) pure dephasing, acting independently on all sites with an equal rate γ. We choose dephasing because it is one of the simplest forms of noise, giving us a single-parameter minimal model that exhibits the desired behaviour. Insofar as dephasing is the appropriate limit of several more realistic noise models, we can expect qualitatively similar effects if more complicated environments are considered. The dephasing superoperator $\mathcal{D}$ is defined through $(\mathcal{D}\rho)_{nm} = -2\gamma\,(1-\delta_{nm})\,\rho_{nm}$ and the resulting complete equation of motion is

$$\dot{\rho} = \mathcal{L}\rho = -\mathrm{i}\left(H\rho - \rho H^\dagger\right) + \mathcal{D}\rho, \tag{4}$$

where the total Hamiltonian is $H = H_0 + H_{\text{atten}}$. We note that this master equation has been solved exactly for the case $\kappa = \mu = 0$ both in the single-particle situation [22, 23] and in the

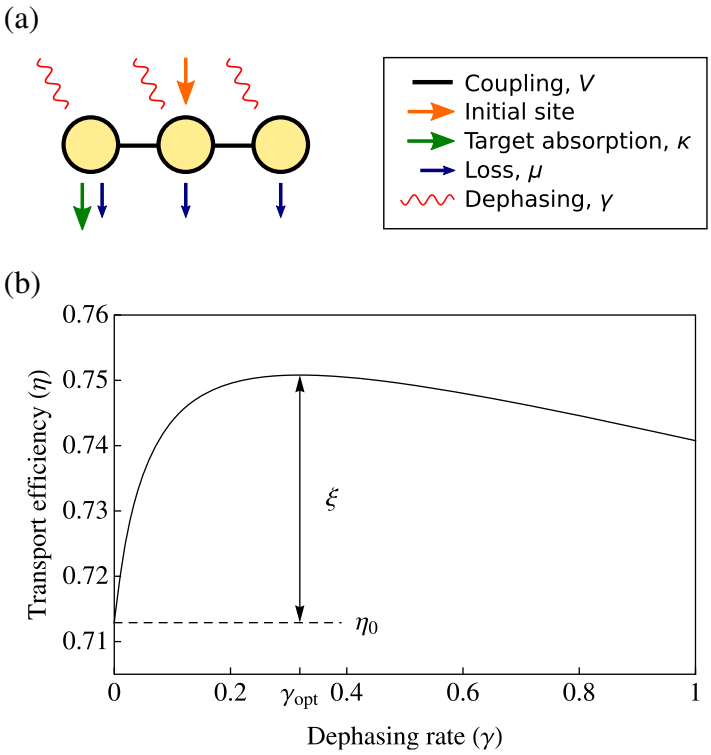

Figure 1. Definition of ENAQT. (a) Three-site chain with the initial site $|2\rangle$ and the trap site $|1\rangle$. (b) Transport efficiency η in the three-site chain, with the trapping rate $\kappa = 0.1$ and the loss rate $\mu = 0.01$. η is maximized at the optimal dephasing rate $\gamma_{\text{opt}} = 0.319$. ENAQT is the magnitude of the enhancement, $\xi = \eta_{\max} - \eta_0$ or in this case, $\xi = 0.038$.

non-equilibrium setting for many particles [24, 25]. In the following, we give a method for the exact (single-particle) solution for any chain length and any κ and μ, allowing us to calculate the efficiency.

The coupling V sets the energy scale, so we can take $V = 1$. Then, at every choice of loss and trapping rates μ and κ, the efficiency η is a function of the dephasing rate γ, see figure 1(b). We observe that if γ is very large, the particle will be localized at its initial site due to the Zeno effect. Therefore, it will not be able to reach the trap before it is lost, meaning that $\eta \to 0$ as $\gamma \to \infty$. Consequently, the maximum transport efficiency $\eta_{\max}$ will occur at a finite $\gamma_{\text{opt}} \geqslant 0$. ENAQT occurs if $\gamma_{\text{opt}} > 0$ and is defined as

$$\xi(\mu, \kappa) = \eta_{\max} - \eta_0. \tag{5}$$

We can now consider efficiency and ENAQT as a function of κ and μ. The following descriptions are all borne out in the example in figure 2, which shows η_0, ξ and γ_{opt} as a function of κ and μ in the finite system of three sites with the trap at one end and the initial site in the middle (see figure 1(a)). Regardless of the number of sites, several limiting cases can be easily understood. Firstly, if $\kappa \ll \mu$, the particle will be lost before it can be trapped, regardless of the amount of dephasing present. Secondly, at large κ, the Hamiltonian term $-i\kappa\,|\tau\rangle\langle\tau|$ presents a high potential barrier for the particle, meaning that it will be largely unable to access the trapping site (this is the case even though the potential is imaginary). Consequently, high

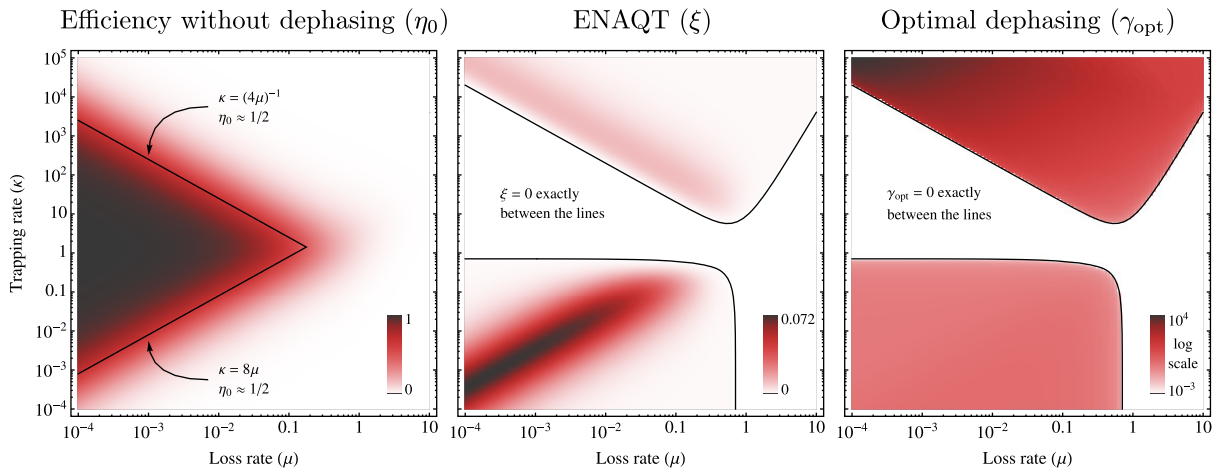

Figure 2. Characterization of ENAQT in the three-site system from figure 1(a). Each of the three parameters defined in figure 1(b) (η_0, ξ, and γ_{opt}) is displayed as a function of trapping and loss rates. (a) High efficiency in the regime with no dephasing is possible only for small loss and intermediate trapping. The two lines indicate the region where the efficiency is about $1/2$, meaning that neither loss nor trapping dominates. They are computed from equation (6) ($\eta_0 = \alpha_0/\beta_0$). (b) Large ENAQT occurs in regions not far from the lines in a, where dephasing can push the balance between loss and trapping in favour of trapping. (c) In the lower left, ξ_{max} occurs when $\gamma_{opt} \approx 0.4151$. On the upper left, strong trapping presents a high potential barrier, meaning that strong dephasing is necessary for ENAQT.

trapping efficiency is possible only in the regime of small μ and intermediate κ (see figure 2(a)). Also, high ENAQT is possible only in this region because outside of it, loss is so dominant that dephasing will be unable to appreciably increase the trapping. This is illustrated in figure 2(b), where it can be seen that ENAQT is large only where η_0 is neither very close to 0 nor very close to 1. That is, ENAQT occurs when neither trapping nor loss is very dominant, meaning that noise can push the balance in favour of trapping.

2. ENAQT on a finite chain

2.1. Analytical solution

Although there is no general solution, ENAQT can be determined analytically in every particular finite system, which is how Plenio and Huelga proved that $\xi = 0$ in the case with the origin and trap at opposite ends of the chain [5]. The solution is by Gaussian elimination (see the appendix), meaning that η is a rational function of γ, κ and μ. For the three-site example in figure 1(a),

$$\eta = \frac{\alpha_2\gamma^2 + \alpha_1\gamma + \alpha_0}{\beta_3\gamma^3 + \beta_2\gamma^2 + \beta_1\gamma + \beta_0}, \tag{6}$$

where $\alpha_2 = 4\kappa\mu$, $\alpha_1 = \kappa(2 + 2\kappa\mu + 8\mu^2)$, $\alpha_0 = \kappa(2\kappa\mu^2 + \kappa + 4\mu^3 + 2\mu)$, $\beta_3 = 8\mu^2(\kappa + \mu)$, $\beta_2 = 4\mu(2\kappa^2\mu + \kappa(8\mu^2 + 3) + 6\mu^3 + 4\mu)$, $\beta_1 = 2\kappa^3\mu^2 + 2\kappa^2\mu(9\mu^2 + 5) + 2\kappa(20\mu^4 + 20\mu^2 + 1) + 6$

$(4\mu^5+6\mu^3+\mu)$, and $\beta_0 = 2\kappa^3(\mu^3+\mu)+\kappa^2(10\mu^4+13\mu^2+1)+\kappa\mu(16\mu^4+29\mu^2+6)+4\mu^2(2\mu^4+5\mu^2+2)$. ENAQT is calculated by maximizing this function with respect to γ. In particular, it can be found that $\partial\eta/\partial\gamma$ can only equal zero if $-\kappa^4\mu+4\kappa^3\mu^4-2\kappa^3\mu^2+2\kappa^3+\kappa^2(20\mu^4+7\mu^2+9)\mu+32\kappa\mu^6+16\kappa\mu^4+7\kappa\mu^2-\kappa+16\mu^7+8\mu^5-4\mu^3-2\mu \geqslant 0$, meaning that there is a region in the (μ,κ) plane in which ENAQT is impossible, as shown in figure 2. In all other cases, ENAQT is strictly positive. The maximum ENAQT is $\xi_{\max} = 7-4\sqrt{3} \approx 0.0718$, obtained as κ and μ simultaneously tend to zero while keeping $\mu = \kappa/2\sqrt{3}$. In that limit, γ_{opt} tends to $\sqrt{\frac{1+\sqrt{3}}{2+8\sqrt{3}}} \approx 0.4151$.

2.2. Limit of small attenuation

It is difficult to form a simple, intuitive picture of ENAQT in this system that remains valid in all parameter regimes, particularly when time scales converge, e.g. at $\kappa \sim 1$ or $\mu \sim 1$. Nevertheless, there is a simple expression for ENAQT in the limit $\kappa,\ \mu \ll 1$. In that case, both attenuation mechanisms are weak and can be treated as perturbations on the dephased quantum dynamics. In particular, because attenuation is slow compared to the quantum dynamics, we assume that we can only consider the average site populations in calculating loss and trapping. In the case with appreciable dephasing, the state of the system will quickly reach a completely mixed state, meaning that each site will host $1/N$ of the remaining population. In particular, the rate at which the particle will be trapped at the trap site will equal κ/N. Similarly, all population will be lost at a rate μ, giving the efficiency

$$\eta_{\text{dephased}} \approx \frac{\kappa/N}{\kappa/N+\mu} = \frac{1}{1+N\mu/\kappa}. \tag{7}$$

In the coherent case, the system eigenstates are $u_j^{(k)} = \sqrt{\frac{2}{N+1}}\sin\frac{\pi jk}{N+1}$ with eigenvalues $\lambda_k = 2\cos\frac{\pi k}{N+1}$. Therefore, the amplitude of site l given an initial site m is

$$U_{lm}(t) = \frac{2}{N+1}\sum_{j=1}^{N}\sin\frac{\pi jl}{N+1}\sin\frac{\pi jm}{N+1}\,\mathrm{e}^{-\mathrm{i}t\cdot 2\cos\frac{\pi j}{N+1}}, \tag{8}$$

which can be used to show that the average population $\bar{P}_{lm} = \lim_{T\to\infty}\frac{1}{T}\int_0^T |U_{lm}(t)|^2\mathrm{d}t$ equals

$$\bar{P}_{lm} = \frac{1}{N+1}\left(1+\frac{1}{2}\delta_{lm}+\frac{1}{2}\delta_{l,N+1-m}\right), \tag{9}$$

where δ_{lm} is the Kronecker delta function. From there we have $\eta_{\text{coherent}} \approx (1+\bar{P}_{lm}^{-1}\mu/\kappa)^{-1}$. For ENAQT, we do not consider the case $l=m$, meaning that there are two situations, depending on whether the trap is opposite the initial site. Because partial recurrences can refocus excitation from the initial site to the opposite site, if the opposite site is the target, $l = N+1-m$, the average target population exceeds $\frac{1}{N}$ and ENAQT is impossible. This explains, at least in the limit of small κ and μ, Plenio and Huelga's observation of the absence of ENAQT in end-to-end transfer. In the transport between sites that are not opposite each other,

$$\xi \approx \frac{1}{1+N\mu/\kappa} - \frac{1}{1+(N+1)\mu/\kappa} > 0. \tag{10}$$

Notably, ξ depends only on the ratio μ/κ. The validity of these approximations is demonstrated in figure 3. The expression is more accurate for large μ/κ because loss, by lowering all the

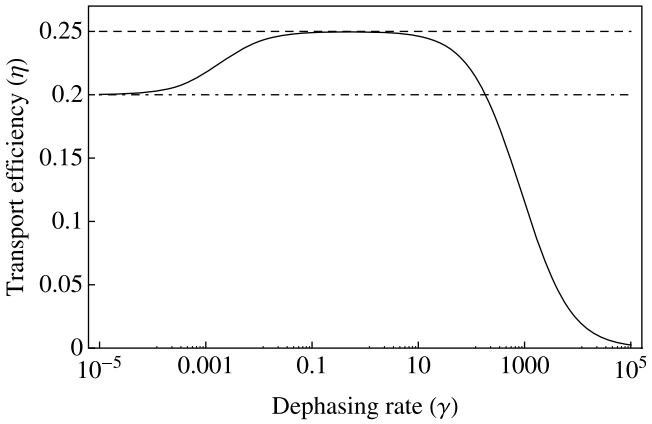

Figure 3. ENAQT in the three-site system from figure 1(a), in the limit of small attenuation, with $\kappa = \mu = 10^{-3}$. As $\gamma \to 0$, the time evolution is merely perturbed coherent evolution, and the efficiency approaches the predicted value of $\frac{1}{5}$ (dash dotted line). As $\gamma \to \infty$, the Zeno effect ensures $\eta \to 0$. In the intermediate regime, $\gamma \sim 1$, the dephasing creates a fully mixed state, for which the predicted efficiency is $\frac{1}{4}$ (dashed line), giving an ENAQT of $\frac{1}{20}$.

amplitudes simultaneously, perturbs the time evolution less than trapping, which affects only one site.

2.3. Other patterns

Several patterns emerge in longer chains and when the locations of the trapping site and the initial site are varied. Table 1 shows the maximum possible ENAQT in chains up to $N = 8$ with all possible combinations of the initial and trap sites. Each entry is calculated by analytically solving the equations of motion and maximizing ξ as a function of κ and μ, as discussed above for the $N = 3$ chain. As we proved above, we can see that ENAQT is possible in all configurations except when the initial site is located opposite the trap. Furthermore, maximum ENAQT increases with increasing N. This is the opposite of the trend predicted by equation (10), and occurs because the high values observed in the table generally occur in the regime of small μ/κ, where the estimate of η_{coherent} fails.

It can also be seen that, regardless of the trap site, $\xi_{\max}$ is equal for situations with initial sites m and $N+1-m$. This is the case even though $\xi(\mu, \kappa)$ is not equal in the two situations in general. In the limit of infinitesimally small κ, μ and γ, where the equality obtains, coherent time evolution proceeds before any appreciable dephasing or loss takes place. Therefore, coherent recurrences can occur, and although the recurrences are imperfect because the eigenvalues λ_k are incommensurable, they become arbitrarily close to perfect after a sufficiently long time. In particular, a particle initialized at m will refocus (arbitrarily close to perfectly) at $N+1-m$ after sufficient time. On the longer time scale of loss, the two initial conditions become indistinguishable.

2.4. High ENAQT in symmetric situations

As shown in table 1, a high ENAQT of $\xi_{\max} = \frac{1}{2}$ occurs if the trap is in the middle of a chain with an odd number of sites, regardless of the initial site. In that case, the full Hamiltonian

Table 1. Analytically calculated maximum ENAQT in a chain with N sites, depending on the initial and trap (τ) sites. ENAQT is not defined if the initial and trap sites coincide (X). All the values with the same N that are equal to three decimal places are exactly equal. $0.072 = 7 - 4\sqrt{3}$ and the rest are roots of more complicated, but known, polynomials.

		Initial site							
N	τ	1	2	3	4	5	6	7	8
3	1	X	0.072	0					
3	2	1/2	X	1/2					
4	1	X	0.083	0.083	0				
4	2	0.083	X	0	0.083				
5	1	X	0.082	0.107	0.082	0			
5	2	1/3	X	1/3	0	1/3			
5	3	1/2	1/2	X	1/2	1/2			
6	1	X	0.080	0.114	0.114	0.080	0		
6	2	0.114	X	0.080	0.080	0	0.114		
6	3	0.080	0.114	X	0	0.114	0.080		
7	1	X	0.077	0.115	0.125	0.115	0.077	0	
7	2	1/4	X	1/4	0.033	1/4	0	1/4	
7	3	0.115	0.077	X	0.125	0	0.077	0.115	
7	4	1/2	1/2	1/2	X	1/2	1/2	1/2	
8	1	X	0.074	0.114	0.128	0.128	0.114	0.074	0
8	2	0.128	X	0.114	0.074	0.074	0.114	0	0.128
8	3	1/3	1/3	X	1/3	1/3	0	1/3	1/3
8	4	0.074	0.128	0.114	X	0	0.114	0.128	0.074

H commutes with the inversion operator P, defined as $P|j\rangle = |N+1-j\rangle$. The initial site $|\tau\rangle$ can be written as an equal superposition of symmetric and antisymmetric states, $|\tau\rangle = \frac{1}{\sqrt{2}}(|S\rangle + |A\rangle)$, where $|S\rangle = \frac{1}{\sqrt{2}}(|\tau\rangle + |N+1-\tau\rangle)$ and $|A\rangle = \frac{1}{\sqrt{2}}(|\tau\rangle - |N+1-\tau\rangle)$. Because $|A\rangle$ is odd, $P|A\rangle = -|A\rangle$ and H commutes with P, $|A\rangle$ remains odd under time evolution. Since the trap site is in the middle, it is even, meaning that the $|A\rangle$ component of $|\tau\rangle$ never gets mapped to the trap site and can therefore not be trapped. In contrast, the $|S\rangle$ component does get trapped. Therefore, the efficiency at zero dephasing is $\eta_0 = \frac{1}{2}$. When dephasing is non-zero, the phase coherence in $|A\rangle$ is lost, meaning that now the particle can be completely trapped. In particular, if $\kappa \gg \mu$, a negligible amount will be lost, meaning that $\eta_{\max} = 1$, giving $\xi = \eta_{\max} - \eta_0 = \frac{1}{2}$.

3. ENAQT on a circle

If the transport takes place on a circle instead of a finite chain, the behaviour is qualitatively the same. We consider here the same situation as above, except that in equation (1), there is an additional term coupling sites $|1\rangle$ and $|N\rangle$.

In the regime of weak attenuation, $\kappa, \mu \ll 1$, as in the chain, $\eta_{\text{dephased}} \approx (1 + N\mu/\kappa)^{-1}$. In the coherent case, the eigenstate amplitudes are $u_j^{(k)} = \frac{1}{\sqrt{N}} e^{2\pi i jk/N}$ with eigenvalues

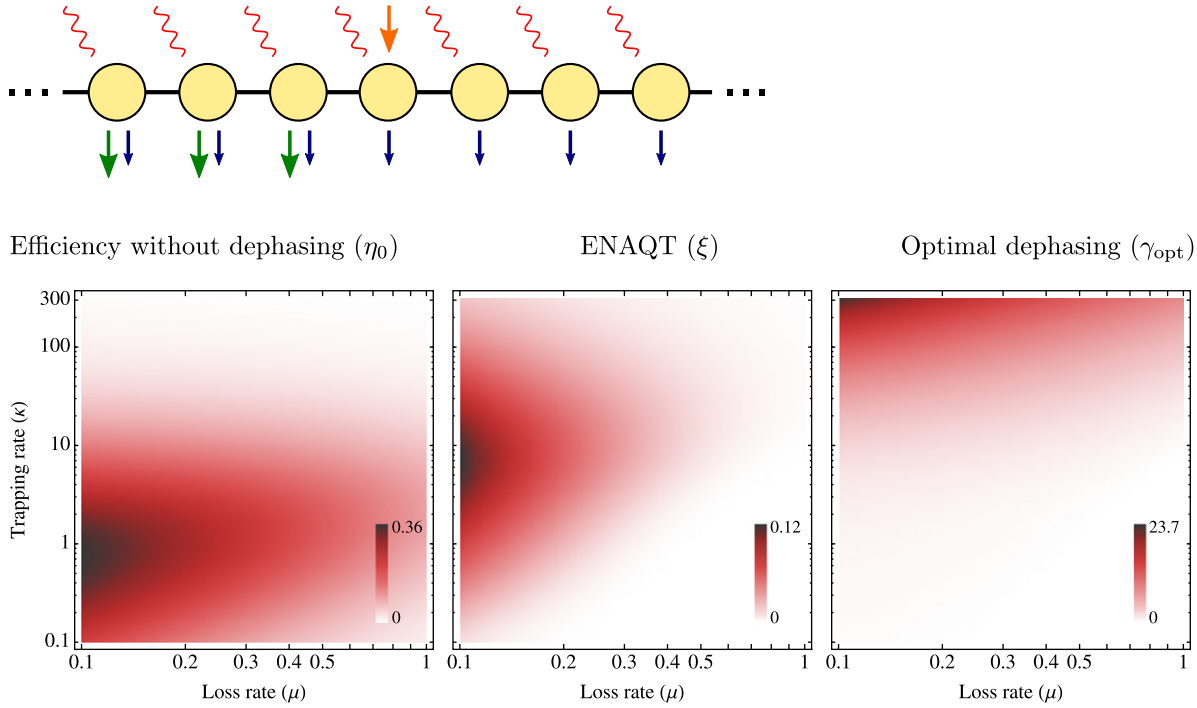

Figure 4. The infinite system (top) and its characterization (bottom). As in the finite chain (figure 2), high η_0 occurs for small loss and intermediate trapping, ENAQT is highest at intermediate η_0 and the dephasing required for ENAQT grows rapidly with increasing κ.

$\lambda_k = 2\cos\frac{2\pi k}{N}$, from where the average population is

$$\bar{P}_{lm} = \begin{cases} \dfrac{1}{N^2}\left(N\left(1+\delta_{lm}\right)-1\right), & N \text{ odd} \\ \dfrac{1}{N^2}\left(N\left(1+\delta_{lm}+\delta_{l,m+N/2}\right)-2\right), & N \text{ even.} \end{cases} \tag{11}$$

Because $\bar{P}_{lm} > \frac{1}{N}$ if $l = m + \frac{N}{2}$, there is no ENAQT if the initial site lies on the opposite side of the circle to the trap. In other cases,

$$\xi \approx \frac{1}{1+N\mu/\kappa} - \frac{1}{1+N^2\mu/(N-1)\kappa} > 0. \tag{12}$$

As in the chain, this expression is more accurate for large μ/κ.

Regardless of the number of sites, the maximum possible ENAQT on the circle is

$$\xi_{\max} = \begin{cases} 0, & \text{the initial and trap sites opposite} \\ \frac{1}{2}, & \text{otherwise.} \end{cases} \tag{13}$$

The situation is much simpler than in the chain, where table 1 is needed. The high value of $\xi_{\max}$ occurs because the circle always has the inversion symmetry required in section 2.4.

4. ENAQT on an infinite chain

ENAQT also occurs—albeit by a different mechanism—in infinite ordered systems. The dephased dynamics of a particle on an infinite chain is well understood in the absence of trapping and loss [17, 26, 27]. In the fully coherent case, $\gamma = 0$, the dynamics is ballistic, while increasing noise converts it into diffusion.

To observe ENAQT, we introduce loss μ everywhere and trapping κ on all sites to the left of the initial site (see figure 4(a)). In the coherent case, there is a sizeable probability that the particle, owing to its ballistic motion, will move far to the right and be lost. In the opposite extreme, $\gamma = \infty$, the particle is completely localized at the initial site by the Zeno effect and is therefore eventually lost. In the intermediate region, ENAQT is possible because decoherence slows down the spreading sufficiently to prevent the rightward-moving component from escaping, but not strongly enough to prevent the particle from diffusing into the trap region.

Figure 4(b) shows numerically computed ENAQT on the infinite chain. The infinite line was represented by sufficiently many sites N to avoid the particle reaching the edges. Because the simulation time and N both scale as μ^{-1}, the computation becomes expensive for small μ, and we have imposed a lower cutoff of $\mu = 0.1$. The largest ENAQT found is $\xi(\mu = 0.1,\ \kappa = 6.3) = 0.1233$. Similar results are obtained with initial sites further from the trapping region. In those cases, ENAQT is smaller because the particle has to travel farther to the trapping region, but remains finite for small μ and intermediate κ. ENAQT tends to zero as $\mu \to 0$, as $\mu \to \infty$ and as $\kappa \to \infty$ for the same reasons as in the finite chain. A question we are not able to answer with numerical simulations is whether ENAQT is for ever exactly zero or merely approaches zero asymptotically in the appropriate limits.

5. Conclusion

We have shown at least two different mechanisms for ENAQT in an ordered system. In the finite lattice with small κ and μ, this is caused by the fact that a dephasing-induced mixed state is more likely to be found at the trap site than a coherently propagated initial state, except when the initial and trap sites are opposite each other. In the infinite lattice, it occurs when dephasing slows down otherwise ballistic transport and prevents a portion of the particle from escaping far away from the trap region. We leave open the questions of whether the various mechanisms of ENAQT (including those in disordered systems) can be understood in a unified picture and how they are influenced by different types of noise, of which pure dephasing is only one limit.

Acknowledgments

We thank Gerard Milburn, Patrick Rebentrost and Andrew White for valuable discussions and Martin Plenio for assistance with the material in the appendix. We acknowledge support from a UQ Postdoctoral Research Fellowship (IK), DARPA (N66001-10-1-4063), and the Camille and Henry Dreyfus Foundation (AAG).

Appendix. Analytical calculation of the efficiency

The initial state of the system $\rho(0)$ can be understood as a vector in a Liouville space of dimension N^2. In order to calculate the efficiency, we augment it to $\tilde{\rho}(0)$ with $N^2 + 1$ entries.

The first N^2 entries we call the state sector, and they are equal to $\rho(0)$, while the final entry, the accumulator, we initialized to $\tilde{\rho}_{N^2+1}(0) = 0$. The Liouvillian $\mathcal{L}$ is likewise modified to $\tilde{\mathcal{L}}$, an $(N^2+1) \times (N^2+1)$ matrix, where the top-left $N^2 \times N^2$ elements are equal to $\mathcal{L}$, and the remainder are set to 0, except for the entry $\tilde{\mathcal{L}}_{N^2+1,\tau'} = 2\kappa$, where $\tau' = 1 + (\tau - 1)(N+1)$ is the coordinate of the population of the trap site τ. That is, $\tilde{\mathcal{L}}$ couples the population of the trap site to the accumulator (but not vice versa) with strength 2κ. Because $\tilde{\mathcal{L}}$ does not couple from the accumulator to the state sector of $\tilde{\rho}(t)$, the time evolution of the state sector under $\tilde{\mathcal{L}}$ is equal to the time evolution of $\rho(t)$ under $\mathcal{L}$. During the evolution, the accumulator increases precisely at the rate $2\kappa\rho_{\tau'}(t)$, meaning that $\tilde{\rho}_{N^2+1}(\infty) = \eta$, while the remaining elements of $\tilde{\rho}(\infty)$ are all reduced to 0. In principle, one could calculate η by calculating $\tilde{\rho}(\infty) = \lim_{t\to\infty} \mathrm{e}^{\tilde{\mathcal{L}}t}\tilde{\rho}(0)$, but this appears to us to be too difficult analytically.

Instead of solving the initial-value problem, we solve a related steady-state equation. We begin by modifying $\tilde{\mathcal{L}}$ to $\tilde{\mathcal{L}}^{\varepsilon}$, which is the same except for $\tilde{\mathcal{L}}^{\varepsilon}_{N^2+1,N^2+1} = \varepsilon$. Then we solve, analytically by Gaussian elimination or otherwise, the linear system of equations

$$\tilde{\mathcal{L}}^{\varepsilon}\tilde{\sigma} = \varepsilon\tilde{\rho}(0). \tag{A.1}$$

Here, $\tilde{\sigma}$ is the steady state in the situation where $\rho(0)$ is being injected into the system at rate ε. In particular, since the total probability of being injected into the system is ε, the fraction $\varepsilon\eta$ must go to the accumulator. Since the accumulator accumulates at a rate $2\kappa\tilde{\sigma}_{\tau'}$, we must have $\tilde{\sigma}_{\tau'} = \varepsilon\eta/2\kappa$. Now, the accumulator component of equation (A.1) is $2\kappa\tilde{\sigma}_{\tau'} + \varepsilon\tilde{\sigma}_{N^2+1} = 0$, from which we can conclude that $\tilde{\sigma}_{N^2+1} = \eta$, meaning that the efficiency can be read out of the solution $\tilde{\sigma}$. The result is independent of ε, meaning that the procedure remains valid in the limit of infinitesimally small ε, where equation (A.1) reduces to a true steady-state equation, $\dot{\tilde{\sigma}} = 0$.

References

[1] Engel G S, Calhoun T R, Read E L , Ahn T-K, Mančal T, Cheng Y-C, Blankenship R E and Fleming G R 2007 Evidence for wavelike energy transfer through quantum coherence in photosynthetic systems *Nature* **446** 782

[2] Panitchayangkoon G, Hayes D, Fransted K A, Caram J R, Harel E, Wen J, Blankenship R E and Engel G S 2010 Long-lived quantum coherence in photosynthetic complexes at physiological temperature *Proc. Natl Acad. Sci. USA* **107** 12766

[3] Collini E, Wong C Y, Wilk K E, Curmi P M G, Brumer P and Scholes G D 2010 Coherently wired light-harvesting in photosynthetic marine algae at ambient temperature *Nature* **463** 644

[4] Rebentrost P, Mohseni M, Kassal I, Lloyd S and Aspuru-Guzik A 2009 Environment-assisted quantum transport *New J. Phys.* **11** 033003

[5] Plenio M and Huelga S 2008 Dephasing-as sisted transport: quantum networks and biomolecules *New J. Phys.* **10** 113019

[6] Gaab K M and Bardeen C J 2004 The effects of connectivity, coherence, and trapping on energy transfer in simple light-harvesting systems studied using the Haken–Strobl model with diagonal disorder *J. Chem. Phys.* **121** 7813

[7] Rebentrost P, Mohseni M and Aspuru-Guzik A 2009 Role of quantum coherence and environmental fluctuations in chromophoric energy transport *J. Phys. Chem.* B **113** 9942

[8] Caruso F, Chin A W, Datta A, Huelga S F and Plenio M B 2009 Highly efficient energy excitation transfer in light-harvesting complexes: the fundamental role of noise-assisted transport *J. Chem. Phys.* **131** 105106

[9] Olaya-Castro A, Lee C, Olsen F and Johnson N 2008 Efficiency of energy transfer in a light-harvesting system under quantum coherence *Phys. Rev.* B **78** 085115

[10] Mohseni M, Rebentrost P, Lloyd S and Aspuru-Guzik A 2008 Environment-assisted quantum walks in photosynthetic energy transfer *J. Chem. Phys.* **129** 174106
[11] Lloyd S 2011 The quantum Goldilocks effect: on the convergence of timescales in quantum transport arXiv:1111.4982
[12] Cao J and Silbey R J 2009 Optimization of exciton trapping in energy transfer processes *J. Phys. Chem.* A **113** 13825
[13] Perdomo A, Vogt L, Najmaie A and Aspuru-Guzik A 2010 Engineering directed excitonic energy transfer *Appl. Phys. Lett.* **96** 093114
[14] Vlaming S M, Malyshev V A and Knoester J 2007 Nonmonotonic energy harvesting efficiency in biased exciton chains *J. Chem. Phys.* **127** 154719
[15] Mohseni M, Shabani A, Lloyd S and Rabitz H 2011 Optimal and robust energy transport in light-harvesting complexes: (II) a quantum interplay of multichromophoric geometries and environmental interactions arXiv:1104.4812
[16] Venuti L C and Zanardi P 2011 Excitation transfer through open quantum networks: three basic mechanisms *Phys. Rev.* B **84** 134206
[17] Hoyer S, Sarovar M and Whaley K B 2010 Limits of quantum speedup in photosynthetic light harvesting *New J. Phys.* **12** 065041
[18] Nalbach P, Eckel J and Thorwart M 2010 Quantum coherent biomolecular energy transfer with spatially correlated fluctuations *New J. Phys.* **12** 065043
[19] Nalbach P, Braun D and Thorwart M 2011 Exciton transfer dynamics and quantumness of energy transfer in the Fenna–Matthews–Olson complex *Phys. Rev.* E **84** 041926
[20] Scholak T, de Melo F, Wellens T, Mintert F and Buchleitner A 2011 Efficient and coherent excitation transfer across disordered molecular networks *Phys. Rev.* E **83** 021912
[21] Scholak T, Wellens T and Buchleitner A 2011 Optimal networks for excitonic energy transport *J. Phys. B: At. Mol. Opt. Phys.* **44** 184012
[22] Esposito M and Gaspard P 2005 Exactly solvable model of quantum diffusion *J. Stat. Phys.* **121** 463
[23] Esposito M and Gaspard P 2005 Emergence of diffusion in finite quantum systems *Phys. Rev.* B **71** 214302
[24] Žnidarič M 2010 Exact solution for a diffusive nonequilibrium steady state of an open quantum chain *J. Stat. Mech.* (2010) L05002
[25] Žnidarič M 2011 Solvable quantum nonequilibrium model exhibiting a phase transition and a matrix product representation *Phys. Rev.* E **83** 011108
[26] Schwarzer E and Haken H 1972 The moments of the coupled coherent and incoherent motion of excitons *Phys. Lett.* A **42** 317
[27] Kendon V 2007 Decoherence in quantum walks—a review *Math. Struct. Comput. Sci.* **17** 1